A Lithium-Ion Battery Degradation Model Agnostic to Cell Chemistry with Integrated State-of-Charge and Temperature Dependence

Bruno Masserano[1], Jorge E. García Bustos[2], Camilo Ramirez[3], Benjamín Brito Schiele[4], Cristóbal E. Allendes[5], Ricardo Salas Espiñeira[6], Sofía Mancilla[7], José Luis Espinoza[8], Aramis Pérez[9], Francisco Jaramillo-Montoya[10], and Marcos E. Orchard[11]

[1,2,3,5,6,7,8,10,11] *Department of Electrical Engineering, Faculty of Physical and Mathematical Sciences, University of Chile, Santiago, Chile*
bruno.masserano@ug.uchile.cl
jorgegarcia@ug.uchile.cl
camilo.ramirez@ug.uchile.cl
cristobal.allendes@ug.uchile.cl
ricardo.salas.e@ug.uchile.cl
sofia.mancilla@ug.uchile.cl
jose.espinoza.v@ug.uchile.cl
francisco.jaramillo@uchile.cl
morchard@ing.uchile.cl

[3] *Advanced Laboratory for Geostatistical Supercomputing (ALGES), Advanced Mining Technology Center (AMTC), Department of Mining Engineering, University of Chile, Chile*
camilo.ramirez@ug.uchile.cl

[4] *Intelligent Sustainable Prognostics Group, Aerospace Structures and Materials Department, Faculty of Aerospace Engineering, Delft University of Technology*
B.A.britoschiele@tudelft.nl

[9] *School of Electrical Engineering, University of Costa Rica, San José, Costa Rica*
aramis.perez@ucr.ac.cr

ABSTRACT

Accurately forecasting lithium-ion battery degradation is essential for safe and cost-effective electrification. This work presents a cycle-wise degradation model that estimates capacity loss based on usage conditions, using only data from a single reference degradation campaign. The model characterizes each equivalent cycle by features extracted from the battery's State of Charge (SoC) profile; specifically, the SoC Range (SR) and Average Swing Range (ASR), and the average ambient temperature. A Similarity-Based Model maps SR and ASR to a normalized expected cycle life, which is further adjusted using a temperature correction factor derived from empirical studies. Unlike approaches requiring chemistry-specific testing, this method assumes, and validates, that cells under similar conditions degrade similarly, allowing generalization across battery types. The degradation rate also incorporates uncertainty through Kernel Density Estimation of observed cycle-to-cycle variations in supervised datasets. Validation was performed using a public lithium-ion degradation dataset, where the model predicted the State of Health (SoH) trajectory of a test cell with a Mean Absolute Error (MAE) of 0.27% of SoH percentage. Because the model uses only operational features readily measured in battery systems, it is practical for integration into battery management systems for real-time SoH tracking, predictive maintenance, and usage optimization. Future work will expand the feature set and refine uncertainty quantification to further improve predictive robustness.

1. INTRODUCTION

Accurately forecasting the health and remaining life of lithium-ion batteries is essential for enabling more sustainable, cost-effective, and safe electrification solutions. This capability is particularly valuable across a wide range of applications, from electric vehicles and drones to stationary storage systems, where batteries are central to performance and lifetime costs. A reliable model for State of Health (SoH) estimation based on real usage conditions improves decision making, allowing the identification of optimal usage profiles (García Bustos et al., 2025), improving the system's safety, and giving more certainty for replacement strategies (Ahwiadi & Wang, 2025).

Lithium-ion batteries are electrochemical systems that continuously degrade over time, far from linear; multiple factors influence this effect, including charge/discharge power rates, idle time, operating temperature, and the State of Charge (SoC) values experienced by the battery (Xiong, Pan, Shen, Li, & Sun, 2020; Vetter et al., 2005). For this study, the impact of operating SoC ranges and ambient temperatures on the degradation rate of batteries is going to be analyzed, along with the development of a cycle-wise degradation model dependent on both of these factors.

The variational effect operating SoC values have on degradation rate is a subject studied before; literature has shown that different SoC ranges affect the battery degradation rate differently (Pérez et al., 2017), also, that operation at high or lower SoC values can asymmetrically degrade the battery (Chowdhury et al., 2024). This introduces the question of what the optimal SoC range is for a given application, or which battery would be ideal to choose when cycle life preservation is of importance in decision-making.

At the same time, batteries have a specific temperature window at which performance is nominal. Studies have shown how operating at extreme temperatures can temporarily affect available capacity and also accelerate battery degradation (Tan et al., 2023). The relation between operating SoC and temperature becomes even more complex, considering that as the battery is used, heat is generated and transmitted to the ambient and the battery itself, which directly impacts the electrical behavior of the system (Rodríguez-Iturriaga et al., 2024), the changes in electrical performance then affect how heat is generated, making both SoC and temperature intrinsically linked. This is a main area of interest in current literature, and integrating these effects into predictive models is key to enabling more informed electro-thermal management, duty-cycle design, and aging-aware scheduling.

Over the past decades, two main approaches have emerged for modeling lithium-ion battery degradation: physics-based models and data-driven models, each with distinct advantages and limitations.

Physics-based models aim to capture the underlying electrochemical mechanisms responsible for capacity fade and internal resistance growth over time. These models often consider phenomena such as the formation of the Solid Electrolyte Interphase (SEI), lithium plating, active material loss, and electrode degradation (Edge et al., 2021). Because they are grounded in first principles, physics-based models provide interpretability and, in some cases, extrapolation capabilities beyond the operating range of the calibration data. However, they typically require detailed knowledge of the cell's internal structure and chemistry, as well as access to parameters that are difficult to measure directly, such as reaction kinetics or electrolyte composition (Han et al., 2019).

In contrast, data-driven models infer relationships between operational variables (e.g., current, SoC, temperature) and battery health indicators by analyzing experimental data. These models range from regressions (Severson et al., 2019) and survival analysis to machine learning techniques such as neural networks (Wang, Zhai, Zhao, Di, & Chen, 2024) and similarity-based methods. Their main advantage lies in their flexibility and ease of deployment, as they require no prior knowledge of internal battery chemistry and can be adapted to different cell types, provided representative data is available. However, their extrapolation ability is generally limited to the range covered in the training dataset, and they tend to offer lower interpretability compared to physics-based approaches.

In recent literature, increasing attention has been given to incorporating operational variables such as temperature, SoC, and current into lithium-ion battery degradation models. These factors are known to have significant and often nonlinear effects on aging behavior. High temperatures can lead to decay of capacity and an increase in internal resistance (Cai et al., 2024). In low-temperature conditions, electrochemical reactions slow down, internal resistance increases, and lithium plating can occur within the cell, all of which contribute to capacity fade and safety risk (Zhang et al., 2021). Similarly, the SoC range and resting SoC influence stress on electrode materials, with shallow cycles and mid-range SoC levels generally reducing degradation (Saxena, Hendricks, & Pecht, 2016). Current levels, particularly high C-rates during charging or discharging, can exacerbate degradation by increasing internal heating and mechanical strain within the electrodes (Saxena, Xing, Kwon, & Pecht, 2019) (Kim, Lee, Shin, Kim, & Chung, 2024).

Despite the industrial relevance of degradation modeling, high-quality degradation data remains scarce; full cycling experiments under controlled conditions can take months to complete for a single cell. As a result, there is a strong need to develop models that can extrapolate from limited datasets, using representative features of usage profiles to estimate degradation across different battery types and applications.

Building on the hypothesis that cells operated under comparable conditions age in comparable ways, we present a cycle-wise, similarity-based degradation model that needs only a single reference degradation curve to generalize to arbitrary SoC and temperature profiles. Each equivalent cycle is summarized by three readily measured features, the SoC range (SR), the Average Swing Range (ASR), and the mean ambient temperature, then matched, via a k-nearest-neighbour search in (SR, ASR) space, to a normalized cycle life derived from the reference data. This estimate is scaled by an empirically fitted temperature factor derived from the work of (Zhou, Qian, Allan, & Zhou, 2011) and blended with a stochastic term learned from repeated aging campaigns, yielding an interpretable degradation rate that can update battery SoH after every cycle without recourse to chemistry-specific parameters.

The contributions of this work are threefold: (1) we formalize the notion of equivalent cycles as a common operational unit, enabling consistent SoH updates across variable usage profiles. (2) We define a degradation model that operates every equivalent cycle using SoC and temperature features; and (3) we generalize this model for any lithium-ion cell using only a single degradation curve as a reference, usually found in the battery's datasheet.

The model is validated using publicly available cycling data from (Pozzato, Allam, & Onori, 2022), demonstrating its effectiveness in estimating SoH over time under realistic usage conditions. Ultimately, this approach supports applications in predictive maintenance, fleet health monitoring, and thermal-aware battery system design.

2. THEORETICAL BACKGROUND

2.1. Similarity-Based Degradation Model

Similarity-based models (SBMs) predict an output by locating past observations that lie close to the query point in a suitable feature space and combining their recorded responses (Cover & Hart, 1967). They require little or no global parameter fitting, making them suitable whenever data are scarce or heterogeneous. In battery research, SBMs have been adopted to translate a small set of aging experiments into health estimates for a wide range of duty cycles, thereby reducing the need for chemistry-specific testing (Berecibar et al., 2016). We build on this idea by encoding every equivalent cycle (The formal definition appears in Section 3) with two physically interpretable descriptors: the SoC range,

$$SR_k = \max(\mathbf{S}_k) - \min(\mathbf{S}_k), \tag{1}$$

and the average SoC,

$$ASR_k = \frac{1}{N}\sum_{i=1}^{N} s_i. \tag{2}$$

The pair (SR_k, ASR_k) defines a point in a two-dimensional *similarity space*.

A single aging campaign conducted under different SoC windows produces a reference table.

$$\mathcal{A} = \{(\mathbf{x}^{(i)}, \eta^{(i)})\}_{i=1}^{M}, \qquad \mathbf{x}^{(i)} = [SR^{(i)}, ASR^{(i)}], \tag{3}$$

where each $\eta^{(i)}$ is the measured capacity-retention factor. To compare cycles of unequal depth of discharge, every $\eta^{(i)}$ is normalised to a full 100 %-depth equivalent cycle:

$$\eta_{\text{eq}}^{(i)} = \left(\eta^{(i)}\right)^{SR^{(i)}/100}. \tag{4}$$

Given a new point $\mathbf{x}_k = [SR_k, ASR_k]$, the k nearest neighbours in $\mathcal{A}$ are found with Euclidean distance. The degradation factor is the distance-weighted mean

$$\eta_k = \frac{\sum_{j\in\mathcal{N}_k} w_j\, \eta_{\text{eq}}^{(j)}}{\sum_{j\in\mathcal{N}_k} w_j}, \qquad w_j = \frac{1}{\|\mathbf{x}_k - \mathbf{x}^{(j)}\|_2 + \varepsilon}, \tag{5}$$

where ε avoids division by zero.

This similarity approach needs only one degradation campaign to build $\mathcal{A}$, which remains agnostic to electrode chemistry, and is light enough for real-time implementation (Severson et al., 2019).

2.2. Degradation and temperature considerations

As Allendes et al. (2024) shows, there is a bidirectional relation between temperature and the electrical variables of a cell, both of which affect degradation rates through different mechanisms. On the one hand, higher temperatures temporarily increase extractable capacity, altering the SoC dynamics for the same usage profile; as a result, degradation differs across temperatures. On the other hand, electrical cycling of the cell generates internal heat due to ohmic and entropic effects, leading to temperature increases which have been shown to significantly accelerate the degradation process (Hou, Yang, Wang, & Zhang, 2020). These two effects lead to the conclusion that, in order to have a model that accurately describes the degradation process, it is necessary to include the considerations of temperature.

While the aforementioned work proposes an electrothermal model and acknowledges the need to consider degradation, it does not show how temperature affects the degradation rate of a cell. Literature establishes a link between degradation and temperature, specifically showing in Zhou et al. (2011, Fig. 6) how the number of available cycles changes as tem-

perature varies. In that article, this is explained through the Arrhenius equation, which states that the chemical reaction rate of a battery Φ depends on temperature through

$$\Phi = \Phi_{\text{ref}} \exp\left(\frac{E_a(\Phi)}{R}\left[\frac{1}{T_{\text{ref}}} - \frac{1}{T}\right]\right), \tag{6}$$

where T_{ref} is the reference temperature, T is the ambient temperature, $R = 8.3144\,\text{J}\,\text{K}^{-1}\,\text{mol}^{-1}$ is the gas constant, and $E_a(\Phi)$ is the activation energy. These changes of the chemical reaction rate then have an effect on the resistance of the film grown on the electrode, which the authors argue is proportional to the changes in capacity, therefore forming a connection between temperature and available cycles.

3. METHODOLOGY

The proposed model estimates the degradation of lithium-ion batteries by computing a degradation rate after each completed duty cycle. This rate, denoted η_k, reflects the irreversible capacity loss associated with the usage conditions observed during the k-th cycle, and is used to update the battery's SoH, as shown in the practical application of the degradation model in Figure 1.

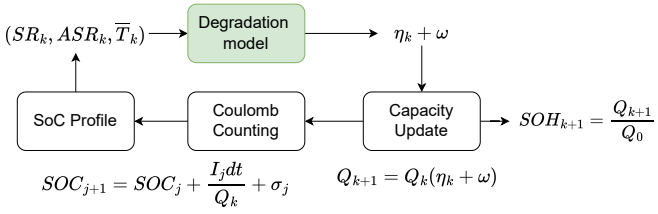

Figure 1. Application-level structure of the degradation model. The SoC profile is generated from a duty cycle, and the degradation rate $\eta_k + \omega$ is applied to update battery capacity and SoH.

The starting point of the methodology is the occurrence of a duty cycle, defined as an operational period during which the battery is actively used (e.g., powering a load, performing vehicle maneuvers, among others). As current is drawn from the battery over time, the SoC decreases according to Equation 7. Through Coulomb counting, the battery's SoC profile can be reconstructed from its current input, resulting in a time-resolved trajectory of SoC values.

$$SoC_{j+1} = SoC_j + \frac{I_j dt}{Q_k} + \sigma_j \tag{7}$$

Once enough energy has been discharged to match the current usable capacity of the battery Q_k, an equivalent cycle is considered complete. At this point, three features are extracted: two related to the SoC values from the coulomb counting and the average ambient temperature during the cycle: the SoC Range (SR_k), defined as the difference between the maximum and minimum SoC values; the Average SoC (ASR_k), computed as the mean SoC throughout the cycle duration; and the Average Ambient Temperature ($\overline{T}_k$), which corresponds to the average environmental temperature experienced during the cycle.

These features form the input to the degradation model, then the degradation rate η_k is computed in two stages, as shown in Figure 2. First, the SR and ASR features are used in a Similarity-Based Model (SBM) to estimate the expected number of cycles to End-of-Life (EoL) ($\mathbf{N}_k$) under the current usage conditions, relative to a nominal full-range profile. This value is then corrected using a temperature-based compensation factor $\gamma_k(\overline{T}_k)$ derived from work in (Zhou et al., 2011), yielding an adjusted equivalent cycle life $\mathbf{N}'_k$, from which the degradation rate η_k is calculated.

Additionally, a stochastic additive noise ω is incorporated into the degradation rate estimate to account for the inherent variability in the aging process and unmodeled phenomena that may affect capacity fade. The noise is modeled as a non-parametric distribution empirically derived from repeated degradation observations under identical cycling conditions from (Pozzato et al., 2022), ensuring the model can reproduce realistic dispersion in SoH trajectories across similar batteries.

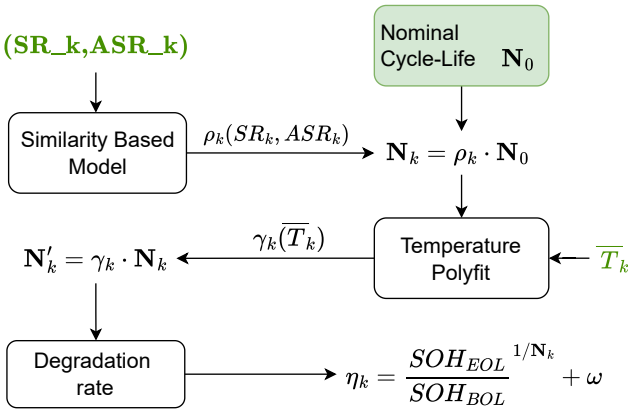

Figure 2. Internal structure of the degradation model. The base degradation rate is computed using a similarity-based method and corrected for ambient temperature.

3.1. Standardization on battery cycle definition

A critical aspect in modeling lithium-ion battery degradation is how to define a "cycle". Traditional definitions based on full charge-discharge cycles typically from 100% to 0% SoC fail to reflect the diversity of usage patterns encountered in real-world applications. In electric vehicles, drones, and energy storage systems, batteries are often used over partial SoC windows, experience irregular discharges, or are cycled under dynamic load conditions. This makes the use of a rigid

full-cycle definition inadequate for generalizable degradation modeling.

To resolve this, we define the concept of an equivalent cycle, which provides a standardized unit of energy throughput independent of the shape or structure of the individual SoC profile. An equivalent cycle is defined as: A cumulative discharge of energy equal to the current full capacity of the battery, regardless of the number or shape of intermediate subcycles that make up the discharge.

In this framework, the model continuously accumulates the discharged energy from the battery. Once this accumulation equals one full discharge of the current SoH-adjusted capacity, an equivalent cycle is considered complete. This approach allows the degradation model to operate consistently across arbitrary usage conditions while preserving physical interpretability.

By design, equivalent cycles decouple the model from assumptions about cycle symmetry or structure. For instance, a full 100%–0% discharge corresponds to exactly one equivalent cycle, whereas four 25%–0% discharges would also accumulate to one equivalent cycle. This makes the equivalent cycle an ideal abstraction for usage-based degradation modeling, enabling accurate SoH updates on a per-cycle basis, even when the underlying SoC trajectory is highly irregular.

3.2. SoC-based degradation rate

Following the methodology proposed in (Pérez et al., 2017), the k-th equivalent cycle is characterized using the (SR_k) and the (ASR_k). These features serve as a compact representation of the electrochemical stress imposed on the battery during that cycle, and for this work, the assumption that these features are sufficient to characterize the entire SoC profile is made. Additional features related to the SoC profile are proposed for future work in this matter.

Here, the SoC-based cycle life $\mathbf{N}_k$ of the battery for the given (SR_k, ASR_k) pair is computed following equation 8.

$$N_k = \rho(SR_k, ASR_k) \cdot N_0 \tag{8}$$

Where $\mathbf{N}_0$ corresponds to a baseline cycle-life of the battery which can be obtained from the datasheet or a single degradation curve from experimental data on the battery and the term $\rho(SR_k, ASR_k)$ to a factor derived from the SBM, which represents the proportion of a base cycle life at $SR = 100$ adjusted to the (SR_k) and (ASR_k) of the current cycle.

The factor ρ is computed via k-Nearest Neighbors approach, where each point in the space is defined from an experimental database in which cells were cycled within fixed SoC windows until their capacity fell to 80% (the EoL criterion), giving the proportions of the base cycle life shown in Table 1.

Table 1. Normalized degradation factors for each SR.

SR	Life Cycle Percent
100-0	1.00000
100-25	0.78750
75-0	1.12525
100-50	0.43750
75-25	0.68750
50-0	1.03125
100-75	0.40625
75-50	0.29700
62.5-37.5	0.28125
50-25	0.62500
25-0	1.00000

The main difference in contribution from the original SBM formulation is that each reference point in the table was associated with a relative degradation factor, designed to multiply a base degradation rate defined by the nominal cycle life in the battery's datasheet. In contrast, our approach uses a normalized representation: each reference point corresponds to the fraction of total cycle life (i.e., number of equivalent cycles to EoL) associated with that SoC condition, relative to a base case of full-range cycling ($SR = 100$). This allows for extrapolating the reference points to be applied to batteries with any arbitrary cycle life, regardless of their chemistry, as long as they remain lithium-ion batteries. These values are presented in Table 1.

As a new equivalent cycle occurs with arbitrary SR and ASR values, the model performs a weighted interpolation using the three nearest neighbors in the feature space. This interpolation yields a new life expectancy value $\mathbf{N}_k$, defined as the estimated number of equivalent cycles the battery could sustain under the current conditions until its EoL.

This formulation enables the degradation model to flexibly adapt to diverse usage conditions, even those not explicitly covered in the original dataset. By expressing the degradation rate in terms of a normalized equivalent cycle life, the model preserves physical interpretability and compatibility across different cell types and duty cycles.

3.3. Temperature-based degradation rate

In addition to SoC-related stressors, the ambient temperature at which a battery operates plays a significant role in its long-term degradation. Elevated temperatures accelerate electrochemical side reactions, increase internal resistance, and promote the growth of passivation layers such as the SEI. This is

also the case for lower temperatures, where lithium dendrites can form, all of which contribute to a faster reduction in usable capacity and a higher risk of thermal runaway (Edge et al., 2021).

To account for these thermal effects, the model incorporates a temperature-dependent correction factor, denoted as $\gamma_k(\overline{T}_k)$, which scales the equivalent cycle life estimated by the SBM $\mathbf{N}_k$. This factor is defined such that:

$$\mathbf{N}'_k = \gamma_k(\overline{T}_k) \cdot \mathbf{N}_k, \tag{9}$$

where $\mathbf{N}_k$ is the uncorrected number of equivalent cycles to EoL estimated by the SBM, and $\mathbf{N}'_k$ is the adjusted value after accounting for the ambient temperature $\overline{T}_k$ experienced during the cycle.

The temperature compensation factor $\gamma_k(\overline{T}_k)$ is derived from the experimental results reported by Zhou et al. (2011), which show a strong nonlinear dependence of cycle life on ambient temperature. In that study, a lithium-ion cell with a nominal life of 2000 cycles at 25°C was observed to degrade more rapidly as the temperature increased, with the cycle life reduced by more than 50% at 55°C, the same was observed for lower temperatures. We extracted this curve and fitted a polynomial approximation to it, producing a continuous mapping from average temperature to a normalized cycle life factor ranging between 0 and 1, so that the resulting compensation curve can be applied to any cell regardless of its nominal cycle life.

The factor $\gamma_k(\overline{T}_k)$ thus represents the proportion of total life that remains at a given average ambient temperature, relative to nominal conditions (typically around 25°C). This compensation is integrated into the degradation model by modifying the life expectancy value passed to the SoC-based degradation rate formula:

$$\eta_k = \left(\frac{\mathrm{SoH}_{\mathrm{EOL}}}{\mathrm{SoH}_{\mathrm{BOL}}}\right)^{1/\mathbf{N}'_k}, \tag{10}$$

where $\mathbf{N}'_k = \gamma_k(\overline{T}_k) \cdot \mathbf{N}_k$ corresponds to the temperature-adjusted cycle life, $\mathrm{SoH}_{\mathrm{EOL}}$ the SoH defined at the EOL of the battery after the $\mathbf{N}_k$ cycles happen and $\mathrm{SoH}_{\mathrm{BOL}}$ the SoH defined at the beginning of life (BoL) of the battery. This temperature-based adjustment ensures that the model captures the acceleration of degradation under both high and low temperature conditions, while preserving compatibility with the normalized framework of the SBM. As a result, the degradation rate η_k for each equivalent cycle reflects both SoC profile features and the thermal stress encountered during operation.

3.4. Uncertainty characterization of the degradation rate

While the proposed degradation model computes a deterministic degradation rate η_k based on the SoC profile and average ambient temperature of each equivalent cycle, experimental evidence shows that degradation is inherently stochastic (Pozzato et al., 2022). Even under tightly controlled cycling protocols, lithium-ion batteries exhibit variability in aging behavior due to internal material heterogeneity, measurement noise, manufacturing inconsistencies, and other unmodeled effects.

To quantify this uncertainty, we analyzed a supervised degradation dataset in which multiple battery cells were cycled under the exact same SoC profile until reaching a predefined EoL condition. The SoH of each cell was periodically measured every few repeated cycles, enabling the empirical calculation of a degradation rate for each observation:

$$\hat{\eta}_j = \left(\frac{\mathrm{SoH_j}}{\mathrm{SoH}_{\mathrm{BOL}}}\right)^{1/\hat{\mathbf{N}}_j} \tag{11}$$

Where $\mathrm{SoH_j}$ correspond to the SoH value reported by the dataset every few repeated equivalent cycles and $\hat{\mathbf{N}}_j$ the accumulated equivalent cycles experienced by each cell until the j-th measure.

In theory, since all cells were subjected to the same repeating duty cycle, the degradation rate η_j should remain constant across cycles. However, the observed values $\hat{\eta}_j$ in Figure 3 displayed significant variation, revealing an underlying distribution of degradation outcomes even under identical conditions.

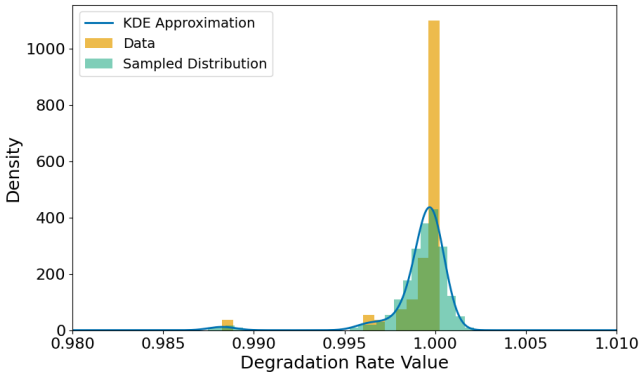

Figure 3. Histogram of observed $\hat{\eta}_j$ values from the degradation dataset (Pozzato et al., 2022).

To characterize this variability, we applied a Kernel Density Estimation (KDE) technique to the empirical distribution of observed $\hat{\eta}_j$ values. The KDE yields a smooth, continuous estimate of the probability density function (PDF) of degradation rates for a fixed cycle type. From this distribution, the

standard deviation σ_η was extracted to represent the intrinsic uncertainty in the degradation process.

This uncertainty was incorporated into the final degradation model by treating the degradation rate η_k calculated by the model as a random variable with an additive stochastic term:

$$\eta_k^{\text{final}} = \eta_k + \omega, \qquad \omega \sim KDE, \tag{12}$$

where η_k is the deterministic degradation rate obtained from SoC and temperature features (as described in Sections 3.2 and 3.3), and ω is a stochastic term derived from the KDE.

This formulation allows the model to not only estimate the expected capacity loss per equivalent cycle but also reflect the range of possible deviations due to factors not captured explicitly by the input features. As such, the uncertainty-aware model provides a more realistic framework for applications in prognostics and risk-informed battery management.

4. CASE STUDY

4.1. Degradation dataset description

To validate the performance of the proposed model using empirical data, both for training and validation phases, the degradation dataset in (Pozzato et al., 2022) provides degradation data for various INR21700-M50T lithium-ion cells with a nominal capacity of 4,850 mAh identified by a code name XY (X being a letter and Y a number). The cells underwent cycling from a fully healthy state down to approximately 91% SoH. The operational cycle implemented for degradation testing is outlined in Table 2.

Table 2. Degradation dataset operational cycle

Step	Action	Termination Condition
1	CC Charge at variable C-Rate	Voltage reaches 4 V
2	CV Charge	Current below 50 mA
3	CC Charge at C/4	Voltage reaches 4.2 V
4	CV Charge followed by 30-min rest	Current below 50 mA
5	CC Discharge at C/4	20 % capacity discharged (80 % SoC)
6	UDDS Discharge	60 % capacity discharged (20 % SoC)

The dataset specifically comprises lithium-ion cells cycled under controlled laboratory conditions, characterized by a constant temperature environment of 25°C. Each cycle includes constant current-constant voltage (CCCV) charging and specific discharge protocols. The discharge phase involves an initial constant current phase down to 80% SoC, followed by a scaled version of the Urban Dynamometer Driving Schedule (UDDS) to simulate real-world urban driving scenarios, continuing down to 20% SoC. The CCCV charging stage varies in current rates among cells, allowing analysis across diverse charging conditions.

Specifically, for validating this particular model, the cycling data of cell W9, the identifier for one of the cells, from the original dataset, was initially utilized to parameterize the model. Critical variables of interest included the number of operational cycles executed and the recorded SoH values throughout the degradation process under these defined operational conditions. Additionally, Incremental Capacity Analysis (ICA) was performed periodically, providing accurate ground-truth capacity measurements, facilitating the interpolation of capacity values for each discharge cycle. Although it is worth noting, from Figure 4, that some ground truth values between 100 and 200 equivalent cycles of the cells used in this case study are missing due to problems with the experiment process.

4.2. Results

After defining the model parameters with cell W9 (training cell), we evaluated performance using cell W10 (validation). The validation process was structured in two phases. First, one of the cells in the dataset was selected to calibrate the degradation model. This involved extracting the reference degradation rates used in the SBM, estimating the temperature compensation curve from ambient data, and computing the uncertainty distribution of η_k based on repeated cyclic SoH measurements. This battery serves as the reference cell and provides all necessary degradation parameters to simulate behavior under different conditions.

In the second phase, a different cell from the dataset was used to evaluate the model's predictive capabilities. The time series of current measurements for this cell was processed using Coulomb counting to reconstruct the SoC profile. As energy was discharged, the simulation tracked the cumulative capacity loss. Every time an equivalent cycle was completed, the SoC profile and ambient temperature during that cycle were used to compute the degradation rate η_k, incorporating both the SBM estimate and the temperature-based correction.

The SoH was updated iteratively after each equivalent cycle, following:

$$\text{SoH}_{k+1} = (\eta_k + \omega) \cdot \text{SoH}_k, \tag{13}$$

where $\omega \sim KDE$ represents the modeled uncertainty extracted from the reference cell's observed degradation variability. The complete degradation curve of the dataset was

calculated repeatedly with Monte Carlo simulations to characterize the uncertainty of the aging process. Figure 4 shows the comparison between the simulated SoH trajectories and the experimentally measured SoH of the validation cell, obtaining a MAE of 0.0027, equivalent to approximately 0.25% SoH error. The results demonstrate that the model is capable of accurately reproducing the degradation trend using only input features derived from operational data (SoC profile and ambient temperature), without requiring multiple full-cycle tests or chemistry-specific models. The predicted EoL point closely matches the actual EoL within a small error margin.

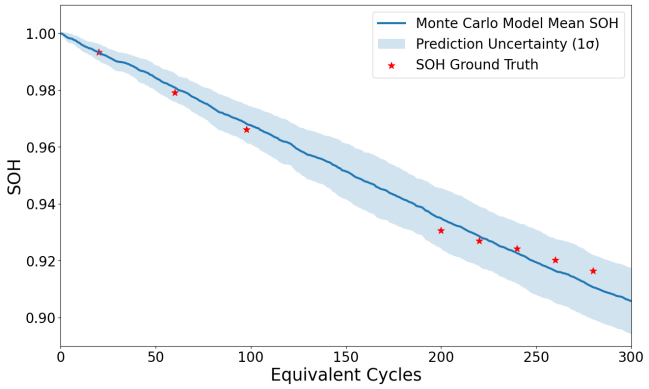

Figure 4. Comparison of predicted SoH from the degradation model vs. measured SoH of the test cell from the degradation dataset.

This validation confirms the model's suitability for practical applications, such as health-aware battery management, usage optimization, and predictive maintenance. Furthermore, the generalizability of the methodology enables its deployment across different battery chemistries and usage profiles, as long as one representative degradation case is available for calibration.

5. CONCLUSION AND FUTURE WORK

This paper presented an interpretable and generalizable degradation model for lithium-ion batteries, capable of estimating capacity loss after each equivalent cycle based on the operating conditions of the battery. By using three simple but informative features from the SoC profile alongside the ambient temperature, the model effectively captures the main drivers of degradation without requiring detailed information about cell chemistry or internal structure.

A key innovation in this work is the use of a normalized SBM, which interprets each SoC condition in terms of its relative cycle life fraction, rather than applying absolute degradation factors. This allows the model to be calibrated from a single degradation dataset and then applied to different usage profiles and battery types, provided they share similar lithium-ion chemistries. The inclusion of a temperature correction factor, derived from empirical degradation trends, enhances the model's sensitivity to thermal effects, while the incorporation of stochastic uncertainty through kernel density estimation acknowledges the real-world variability of battery aging. The predicted EoL point showed a MAE of approximately 0.25%, confirming the model's accuracy and practical utility.

Because the model relies only on features that can be derived from current and temperature measurements commonly available in Battery Management Systems, it can be seamlessly integrated into existing frameworks for SoH estimation, Remaining Useful Life (RUL) prediction, and health-aware energy management. These characteristics make the approach especially attractive for fleet-level optimization, predictive maintenance, and long-term reliability assessment.

Future work will focus on extending the model by incorporating additional features beyond SR and ASR, such as current magnitude, rest times, and voltage windows, which are known to influence degradation. Furthermore, we aim to explore uncertainty quantification more rigorously, including additional degradation datasets for the training process and the use of Bayesian or probabilistic machine learning techniques.

ACKNOWLEDGMENT

This work was supported in part by ANID FONDECYT 1250036, Advanced Center for Electrical and Electronic Engineering, ANID Basal Project AFB240002. The work of Jorge E. García Bustos has been supported by ANID-PFCHA/Doctorado Nacional/2022-21221213. Camilo Ramírez is supported by ANID-Subdirección de Capital Humano/Magíster-Nacional/2023 - 22230232 master's scholarship and grants of ANID AFB230001 Advanced Mining Technology Center and FONDEF TA24I10053. The work of A. Perez was supported by the University of Costa Rica under research project 322-C1-467. The authors also gratefully acknowledge the Department of Electrical Engineering, Faculty of Physical and Mathematical Sciences, University of Chile, for financial assistance through its 2025 International Conference Grant Program.

REFERENCES

Ahwiadi, M., & Wang, W. (2025, 1). Battery health monitoring and remaining useful life prediction techniques: A review of technologies. *Batteries*, *11*, 31. doi: https://doi.org/10.3390/batteries11010031

Allendes, C., Beltrán, A., García, J. E., Troncoso-Kurtovic, D., Masserano, B., Brito Schiele, B., ... Rangarajan, S. (2024, nov). Modeling and simulation of thermal effects on electrical behavior in lithium-ion cells. *Annual Conference of the PHM Society*, *16*(1). doi: https://doi.org/10.36001/phmconf.2024.v16i1.4080

Berecibar, M., Gandiaga, I., Villarreal, I., Omar, N., Van Mierlo, J., & Van den Bossche, P. (2016). Critical review of state of health estimation methods of li-ion

batteries for real applications. *Renewable and Sustainable Energy Reviews*, *56*, 572-587. doi: https://doi.org/10.1016/j.rser.2015.11.042

Cai, Q., Ji, Q., Chen, X., Wang, T., Li, L., Yuan, Q., ... jun Cheng, Y. (2024, 10). Comprehensive study of high-temperature calendar aging on cylinder li-ion battery. *Chemical Engineering Science*, *298*. doi: https://doi.org/10.1016/j.ces.2024.120355

Chowdhury, N. R., Smith, A. J., Frenander, K., Mikheenkova, A., Lindström, R. W., & Thiringer, T. (2024, 1). Influence of state of charge window on the degradation of tesla lithium-ion battery cells. *Journal of Energy Storage*, *76*, 110001. doi: https://doi.org/10.1016/j.est.2023.110001

Cover, T., & Hart, P. (1967). Nearest neighbor pattern classification. *IEEE Transactions on Information Theory*, *13*(1), 21-27. doi: https://doi.org/10.1109/TIT.1967.1053964

Edge, J. S., O'Kane, S., Prosser, R., Kirkaldy, N. D., Patel, A. N., Hales, A., ... Offer, G. J. (2021, 4). *Lithium ion battery degradation: what you need to know* (Vol. 23). Royal Society of Chemistry. doi: https://doi.org/10.1039/d1cp00359c

García Bustos, J. E., Baeza, C., Schiele, B. B., Rivera, V., Masserano, B., Orchard, M. E., ... Perez, A. (2025, 2). A novel data-driven framework for driving range prognostics in electric vehicles. *Engineering Applications of Artificial Intelligence*, *142*, 109925. doi: https://doi.org/10.1016/j.engappai.2024.109925

Han, X., Lu, L., Zheng, Y., Feng, X., Li, Z., Li, J., & Ouyang, M. (2019, 8). *A review on the key issues of the lithium ion battery degradation among the whole life cycle* (Vol. 1). Elsevier B.V. doi: https://doi.org/10.1016/j.etran.2019.100005

Hou, J., Yang, M., Wang, D., & Zhang, J. (2020, Feb). Fundamentals and challenges of lithium ion batteries at temperatures between -40 and 60 °C. *Advanced Energy Materials*, *10*(18). doi: https://doi.org/10.1002/aenm.201904152

Kim, D. H., Lee, J., Shin, K., Kim, K. B., & Chung, K. Y. (2024, 8). Empirical capacity degradation model for a lithium-ion battery based on various c-rate charging conditions. *Journal of Electrochemical Science and Technology*, *15*, 414-420. doi: https://doi.org/10.33961/jecst.2024.00241

Pozzato, G., Allam, A., & Onori, S. (2022, 4). Lithium-ion battery aging dataset based on electric vehicle real-driving profiles. *Data in Brief*, *41*, 107995. doi: https://doi.org/10.1016/j.dib.2022.107995

Pérez, A., Quintero, V., Rozas, H., Jaramillo, F., Moreno, R., & Orchard, M. (2017). Modelling the degradation process of lithium-ion batteries when operating at erratic state-of-charge swing ranges. In *2017 4th international conference on control, decision and information technologies (codit)* (p. 0860-0865). doi: https://doi.org/10.1109/CoDIT.2017.8102703

Rodríguez-Iturriaga, P., García, V. M., Rodríguez-Bolívar, S., Valdés, E. E., Anseán, D., & López-Villanueva, J. A. (2024, 8). A coupled electrothermal lithium-ion battery reduced-order model including heat generation due to solid diffusion. *Applied Energy*, *367*, 123327. doi: https://doi.org/10.1016/j.apenergy.2024.123327

Saxena, S., Hendricks, C., & Pecht, M. (2016, 9). Cycle life testing and modeling of graphite/licoo2 cells under different state of charge ranges. *Journal of Power Sources*, *327*, 394-400. doi: https://doi.org/10.1016/j.jpowsour.2016.07.057

Saxena, S., Xing, Y., Kwon, D., & Pecht, M. (2019, 5). Accelerated degradation model for c-rate loading of lithium-ion batteries. *International Journal of Electrical Power and Energy Systems*, *107*, 438-445. doi: https://doi.org/10.1016/j.ijepes.2018.12.016

Severson, K. A., Attia, P. M., Jin, N., Perkins, N., Jiang, B., Yang, Z., ... Braatz, R. D. (2019, 3). Data-driven prediction of battery cycle life before capacity degradation. *Nature Energy*, *4*, 383-391. doi: https://doi.org/10.1038/s41560-019-0356-8

Tan, S., Shadike, Z., Cai, X., Lin, R., Kludze, A., Borodin, O., ... Yang, X.-Q. (2023, 12). Review on low-temperature electrolytes for lithium-ion and lithium metal batteries. *Electrochemical Energy Reviews*, *6*, 35. doi: https://doi.org/10.1007/s41918-023-00199-1

Vetter, J., Novák, P., Wagner, M., Veit, C., Möller, K.-C., Besenhard, J., ... Hammouche, A. (2005, 9). Ageing mechanisms in lithium-ion batteries. *Journal of Power Sources*, *147*, 269-281. doi: https://doi.org/10.1016/j.jpowsour.2005.01.006

Wang, F., Zhai, Z., Zhao, Z., Di, Y., & Chen, X. (2024, 12). Physics-informed neural network for lithium-ion battery degradation stable modeling and prognosis. *Nature Communications*, *15*. doi: https://doi.org/10.1038/s41467-024-48779-z

Xiong, R., Pan, Y., Shen, W., Li, H., & Sun, F. (2020, 10). Lithium-ion battery aging mechanisms and diagnosis method for automotive applications: Recent advances and perspectives. *Renewable and Sustainable Energy Reviews*, *131*, 110048. doi: https://doi.org/10.1016/j.rser.2020.110048

Zhang, G., Wei, X., Han, G., Dai, H., Zhu, J., Wang, X., ... Ye, J. (2021, 2). Lithium plating on the anode for lithium-ion batteries during long-term low temperature cycling. *Journal of Power Sources*, *484*. doi: https://doi.org/10.1016/j.jpowsour.2020.229312

Zhou, C., Qian, K., Allan, M., & Zhou, W. (2011). Modeling of the cost of ev battery wear due to v2g application in power systems. *IEEE Transactions on Energy Conversion*, *26*(4), 1041-1050. doi: https://doi.org/10.1109/TEC.2011.2159977